Self-Current Sensing Intelligent DC Motor Drive using Embedded System for Fuel Cell Application

[1]Shweta Singh, [2]Anurag Rai, [3]C.K. Dwivedi
[1]Research Scholar, [2]Associate Professor, 3Professor
[1]Research Scholar, [2]Research Scholar, [3]Professor
Electronics and communication department, University of Allahabad,
Alahabad-211002, U.P., India

Abstract : ***Self current sensing in an intelligent or robotic system, describes the technique where a single element shares both sensing and actuation, which reduce cost and complexity of the system with reduced power consumption. Hence, it is suitable for robotic systems powered by battery or fuel cell. Moreover, self sensing is suitable for situations where implementation of sensor is not feasible. The objective of the research is to design a self current sensing (SCS) intelligent DC motor drive circuit using embedded systems to detect mechanical limit as well as to protect the circuit from overload current. A DC drive circuit is designed with a controller contains an on-chip analog comparator. The proposed circuit is designed and verified with 12 volt permanent magnet brushed DC motor.***

IndexTerms - self current sensing; driver circuit; fuel cell; no-load current; stall torque.

I. INTRODUCTION

Nowadays, intelligent or robotic systems are an essential part in military and security tasks, health sector, domestic services, means of access and exploration of remote or dangerous places, in the industry (cottage, car, heavy, iron and steel) to increase the productivity and the efficiency [1]. Hence, It is desirable to develop energy saving and self protected system for these chores. Many tactics are used for energy consumption minimization in robotic systems such as usage of energy efficient equipments or renewable energy sources and optimal hardware selection [2]. Most commonly humanoid robots and small mobile robots are powered with batteries or sometimes with internal combustion engines. In a few cases, solar photovoltaic panels [3] are used. Though Combustion engines have high power and high energy, but are noisy and produce toxic exhaust that makes them unsuitable for most applications. Because of the requirement of large surface areas and uniform insolation, Solar panels are rarely used in robotic applications. Hence, rechargeable batteries are currently the power source of choice in these systems. Many researchers [4] have been reported in improvement of battery technology. But the battery needs an external electrical power source to charge, and this is a limitation to the mobility of the device because it can only be used with an existing electrical source. Therefore, it could not meet the mission needs of long duration in field environment and hence, new means for powering ground robots need to be considered.

On the other hand, fuel cells provide an efficient and clean mechanism with offering longer operating duration and operating on a much wider range of temperature [5]. A fuel cell is an electrochemical device that converts the chemical energy of a fuel (Hydrogen and hydrocarbon) directly into electrical energy. It has four major parts i.e. anode, cathode, electrolyte and the external circuit. At the anode, hydrocarbon fuel is oxidized into ions and electrons, while at the cathode oxygen is reduced to oxide species and reacts to form water. According to the choice of fuel and electrolyte, fuel cells are mainly consisted of: Alkaline fuel cell (AFC), Phosphoric acid fuel cell (PAFC), Solid oxide fuel cell (SOFC), Molten carbonate fuel cell (MCFC), Proton exchange membrane fuel cell (PEMFC), Direct methanol fuel cell (DMFC) and biofuel cell [6-8].

AFCs contain alkaline electrolyte potassium hydroxide (KOH) in water based solution and consume pure hydrogen as fuel to generate electricity. NASA first used AFCs in shuttle missions for space applications. They are employed in submarines, boats, forklift trucks and niche transportation applications [9]. PAFCs use liquid phosphoric acid as an electrolyte. The PAFCs were targeted initially for terrestrial commercial applications with CO2 containing air as the oxidant gas and pure hydrogen or hydrocarbons as the primary fuel for power generation. SOFCs operate at very high temperature of 1000^{o}C with ceramic electrolyte and use hydrogen containing gas as fuel. They are mostly used for large scale stationary power generation. MCFCs are based on a mixture of molten salts that act as an electrolyte suspended in a porous, chemically inert ceramic lithium aluminium oxide ($LiAlO_2$) matrix. They are high temperature fuel cells, utilize gasified coal and natural gas to produce electricity. MCFCs are used in coal-based power plants in electrical utility, industrial and military applications. Proton exchange membrane fuel cells (PEMFC), or polymer electrolyte membrane fuel cells consist of solid polymer form proton conducting cast and at the anode, hydrogen is oxidized to liberate two electrons and two protons. The electrons travel through the electronic circuits, whereas protons are conducted from the catalyst layer through the proton exchange membrane. They have the largest range of applications, especially regarding automotive and vehicular transport. DMFC is promoted type of the PEMFCs in which the solution of methanol and water is fed to the anode as fuel. It is a suitable source of power for portable applications due to its ease of fuel delivery, storage, operation at low temperature and lack of humidification requirements, as well as its reduced design complexity and high power density [10-12]. Biofuel employs biocatalysts such as a microbe, enzyme or even organelle interacting with an electrode surface. Biofuel cells are implantable power supplies for sensors, pacemakers and for small portable power devices (wireless sensor networks, portable electronics, etc [13-14].

Fuel cells have also been proposed for various robotic and ground applications such as powering unmanned underwater vehicles [15], humanoid robots [16], hopping robots [17] and field robots [18]. Wang and Lan [19] elaborated rehabilitation aids products on the power requirements, and from the categories of rehabilitation aids such as mobile aids products, rehabilitation robotics and intelligent home products details their advantages and market prospects of the fuel cell. Thangavelautham et.al. [20] suggested that Proton Exchange Membrane (PEM) fuel cells can be developed as power supply for small mobile robots performing long duration missions. Wilhelm, Surgenor and Pharoah [21] converted a power source from conventional lead acid battery to a hydrogen fuelled

PEM micro fuel cell. They showed that the performance of the micro fuel cell was matched to the conventional battery. But when a robot is required to safely interact with a physical environment, a force/torque sensor is required to regulate the interaction forces at the end effectors [22]. Autonomous and humanoid robots should be capable of coexisting with humans in dynamical environments. Thus, it is required to control their reaction forces, when interacting with objects that belong to their operative space or when unpredicted events occur [23]. Where, grasping incorporate an essential mechanism in an autonomous robotic manipulation system operating in human environments. This requires sensors and actuators to generate and measure external forces [24].

Self current sensing (SCS) describes the technique where a single element shares both sensing and actuation. It reduces the number of sensing and actuation devices, and associated power, wiring and interfacing [25]. Hence, this technique is reliable for any grasping mechanism involving DC motor as the actuator, with additional advantages of robustness and reduction in cost and complexity. It is also suitable for the system where the inclusion of sensors is not feasible. The prominence of this paper is the development of self current sensing (SCS) intelligent DC motor drive for robotics or intelligent system by designing a simple electronic circuit powered by battery or fuel cell. The proposed scheme operates on current feedback mechanism which is system independent and compatible with any DC motor driven system. In this paper, microcontroller based DC drive circuit is designed where the microcontroller contains an on-chip analog comparator to compare the reference voltage and the voltage across the low value resistance, which is connected in series with the motor. The stall-Torque and no-load characteristics of DC motor are taken as a comprehensive study to set the reference voltage. Experimental results attained validate the proposed self-sensing scheme. The performance of the designed circuit is verified with 12V permanent magnet brushed DC motor.

II. MECHANICAL LIMIT SENSING

When a DC motor based mechanism reaches to the mechanical limit (or hindrance) meant for the system with continuous supply of electric power, the motor current rises sharply. For example, when a DC motor based autonomous robotic manipulator grasps an object tightly, the motor current raises due to the external torque generated by the gripping. This raising current can damage the motor or the driving circuit and could harm the object that is gripped. Generally, sensors are used to sense the mechanical limit or the end of travel and the information obtained from the sensor is used to control the motor. But, these sensors add together the extra circuitry, cost and electric power consumption to the system.

In SCS technique, the actuator or the driving circuit acts as both a sensor and actuator and measurable parameter of the actuator provides sensing information. Therefore, it reduces the cost, power consumption and complexity of the system. In this technique, the motor current is continuously compared with reference value and as motor current raises from this set value, the action of the motor is controlled i.e. it can be stopped or the direction can be changed. In the present work, for extracting the motor current, a low-side current sensing resistor of low value is used, because of its low cost and high measurement accuracy [26-27]. The current sensing resistor is a type of current to voltage converter. As shown in Figure 1, the current sensing resistor RSENSE is connected in between the load and ground to sense the load current I_{LOAD}.

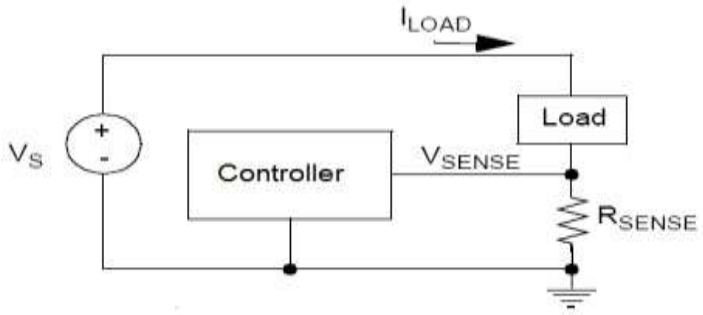

Figure 1: Load current sensing through the low-side current sensing resistor R_{SENSE}.

III. SELF CURRENT SENSING (SCS) CIRCUIT

A self current sensing circuit for DC motor based mechanism is shown in Figure 2. The circuit is designed to control the motor action according to the output of the on-chip analog comparator which compares the reference voltage at the inverting pin to the voltage across the current sensing resistor which is fed to the non-inverting pin. Hence, it reduces the need of external comparator and analog to digital converter. The voltage V_{SENSE} across the current sensing resistor R_{SENSE}, which converts the motor current to corresponding voltage, is given in Equation (1), as

$$V_{SENSE} = I_{LOAD} \times R_{SENSE} = I_{LOAD} \quad (1)$$

The self current sensing (SCS) DC motor drive circuit consists of a Brushed DC motor M, a MOSFET Q2 for driving the motor, Q1 transistor for driving MOSFET, freewheeling diode D3, programmable shunt regulator D1, current sensing resistance R_{SENSE}, potentiometer R3 and resistance R4 as a voltage divider across the programmable shunt regulator. The 89C2051 controller (Atmel) with on-chip analog comparator is used to control the circuit.

In order to set the reference voltage at the non-inverting pin of the on-chip comparator, the prototype DC motor characteristic is observed with no external load and in-stall condition as shown in Figure 3. The self current sensing DC motor drive circuit is designed and tested with 12V, 60 RPM brushed permanent magnet DC motor with gearbox, at different settings of reference voltages by varying the potentiometer R3. The reference voltages can be configured to voltage more than equivalence voltage to no load current and less than the maximum permitted equivalent value of armature current. The whole circuit is powered by a 9 V general purpose battery with 5V voltage regulator.

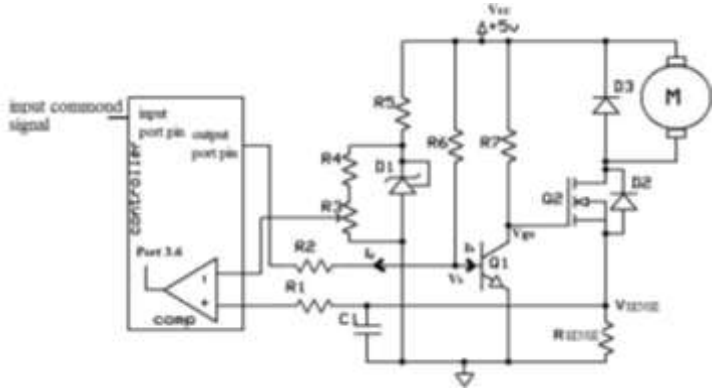

Figure 2: Self current sensing DC motor drive circuit

(a) (b)

Figure 3: The experimental setup for: (a) no external load characteristic; (b) stall condition.

a) No external load characteristic

The no-load characteristic of the 12V, 60RPM brushed permanent magnet DC motor with gearbox was observed by connecting 10Ω (20 Watt) in series with the motor and current controlled voltage source (Figure 3(a)). The voltage from the source, voltage across the 10Ω resistance and motor voltage V_T was observed with a digital multimeter. From these observations, the back electromotive force (EMF) E_b, is calculated from Equation (2).

$$E_b = V_T - I_a R_a \quad (2)$$

The armature current I_a has calculated from the voltage observed across the 10Ω resistance and the value of R_a has calculated from the current verses terminal voltage characteristic of the DC motor in blocked rotor or stall condition. Figure 4(a) illustrates the no-load terminal voltage and armature current characteristic of the DC motor. Until the source voltage reached to more than 0.8V, the motor did not respond and showed linear voltage current characteristic. With further increasing the source voltage, the motor current dropped to 22mA from 40mA and the motor started the rotations. The maximum no load current at 5V and 12V terminal voltage was 25mA and 48mA. Figure 4(b) shows the variation of the back electromotive force (EMF) E_b with angular velocity ω at the DC motor shaft. It gives that E_b is linearly proportional to ω as shown in Equation (3).

$$E_b = 2\,\omega - 0.016 \quad \text{(calculated by MATLAB R2012a)} \quad (3)$$

The motor constant K_e at the shaft of the geared motor is found by taking the derivative of Equation (3), as shown in Equation (4).

$$dE_b/d\omega = 2 \text{ volt sec/radian} = K_e \quad (4)$$

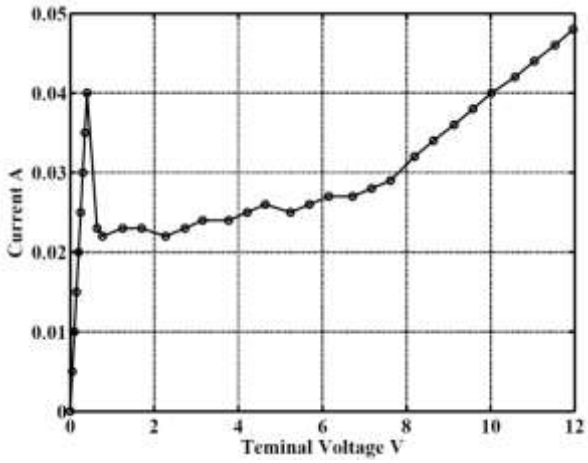

(a)

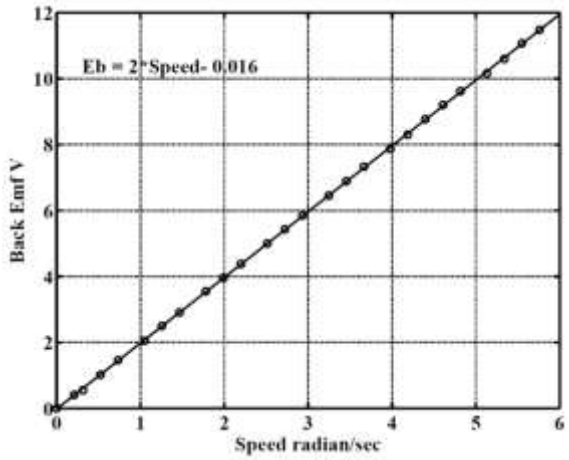

(b)

Figure 4: No load characteristics of the DC motor (a) current verses terminal voltage and (b) E_b verses rotational speed.

b) Stall Condition

Figure 3(b) shows the experimental setup for the observations in a stall condition. In this setup, a 0- 5 Kg spring balance clipped on a nail was tied horizontally through a thread to the shaft of the motor. The source voltage was varied until the motor ran. The voltage across the 10Ω resistance and motor voltage was measured. As the motor started, it pulled the spring balance and the thread was wrapped over the shaft. After some time as the tension force applied by spring balance on the string reached to the motor torque, the motor was blocked. The reading of spring balance, voltage across the 10Ω resistance and motor voltage was measured at the set source voltage. For the next observation, the motor was disconnected to the voltage source and the source voltage preset to next value. The spring balance reading made zero by releasing the wrapped thread. Several observations were taken for different values of source voltages, up to maximum permissible load current.

Figure 5(a) shows the terminal voltage verses motor current characteristic in blocked rotor condition (due to friction and external torque through spring balance), up to maximum load current of the prototype DC motor (i.e. 300mA). Figure 5(b) shows the variation of stall torque T_{stall} with motor current I_a at the DC motor shaft and expression is given in Equation (5). The torque constant K_T at the shaft of the geared motor is obtained from Equation (6)

$$I_a = 2\, T_{stall} + 0.037 \quad (5)$$

$$dT_{stall} / dI_a = 0.5 \text{ Nm/A} = K_T \quad (6)$$

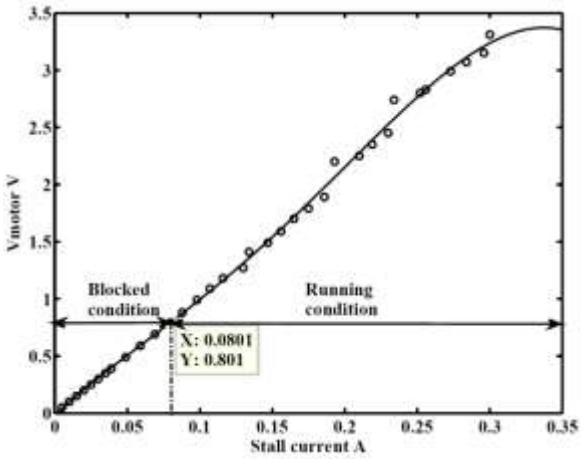

(a)

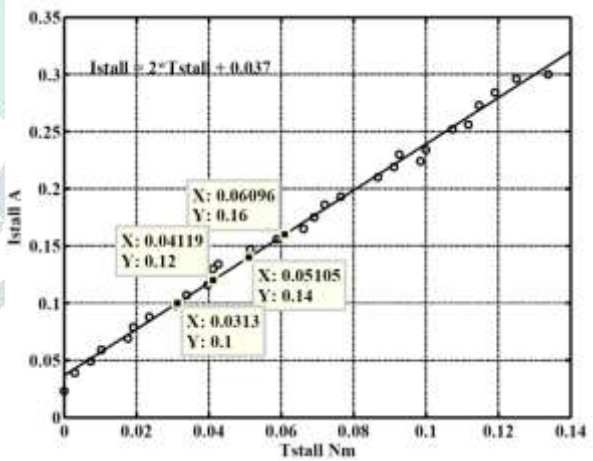

(b)

Figure 5: Stall Condition (a) Terminal Voltage verses stall Current; (b) Stall torque verses current.

IV. EXPERIMENTAL RESULTS AND DISCUSSION

The experiments were conducted to examine the performance of the designed self current sensing (SCS) intelligent DC motor drive circuit using AT89C2051 for detecting the mechanical limit or overload current and to control the action of the motor according to the sensed current. Figure 6 shows the designed experimental circuit of SCS. In order to verify the designed circuit performance, a 12V, permanent magnet brushed DC motor with gearbox was connected across the freewheeling diode D3, which is used for protecting the driver circuit from sudden voltage spikes, due to inductive nature of the motor. A general purpose 9V battery with LM7805 voltage regulator was used as 5V power supply, in the circuit. The reference voltage at inverting pin of the on-chip comparator of the controller (pin 1.1) was set to different fixed voltages by varying the settings of potentiometer R3. With the power on, the output port pin connected to the base of transistor Q1 was 1 i.e. 5V and it worked in saturation region with current $I_b = V_{cc}/R2$, $I_p=0$ and $V_{gs}=0$V. Therefore the MOSFET Q2 did not conduct and the motor was blocked in that condition. As the value of R_{SENSE} is 1Ω, hence the V_{SENSE} is equal to the magnitude of the motor

current I_a. The fixed voltage across programmable voltage regulator D1 is 2.5mV, R4 is 18KΩ and R3 is 0 - 4.7KΩ. The V_{ref} can vary from 0 to 0.517mV by varying the setting of R3. Based on the no-load and stall characteristics of the motor, the V_{ref} value could be set in between 25mV and 300mV. The input command and the on-chip comparator output port pin 3.6 was continuously checked through the software and the motor status was changed accordingly. From Fig. 1, as the controller is getting the command to run the motor, the output port pin is made 0 with current $I_p=V_{cc}/(R2+R6)$, I_b=0A and Q1 is working in cut off region i.e. V_{gs}=5V. In this condition, MOSFET drives the motor till $V_{SENSE}<V_{ref}$ or next input command. The stall condition experimental setup was used to test the SCS circuit. With the application of external load (spring balance), the motor torque is increased continuously and consequently the motor current I_a and voltage V_{SENSE}. While $V_{SENSE}>V_{ref}$, motor stops rotations.

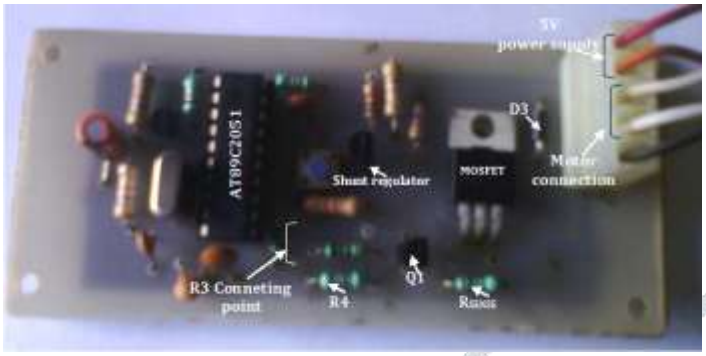

Figure 6: Experimental circuit of SCS.

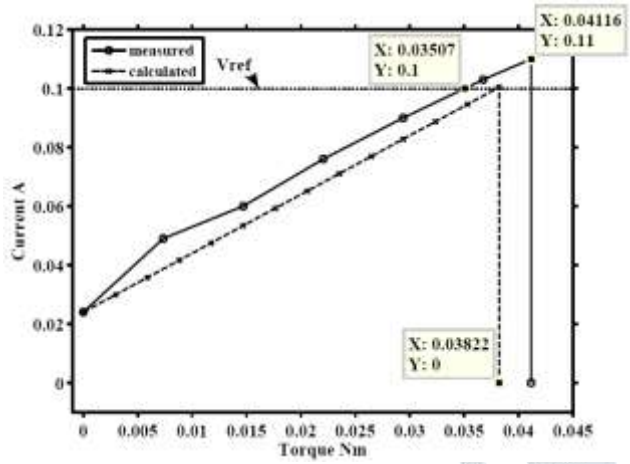

(a)

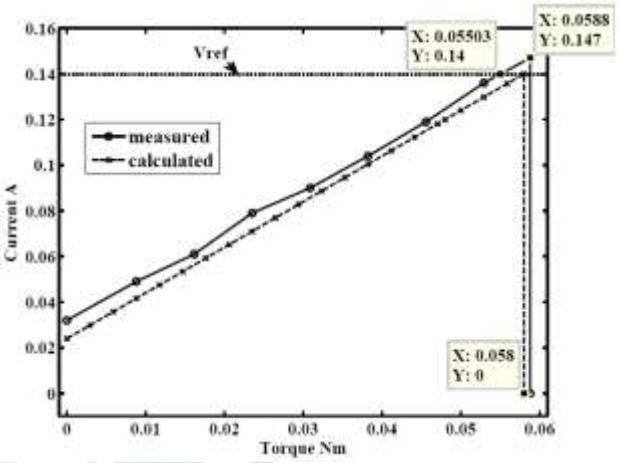

(c)

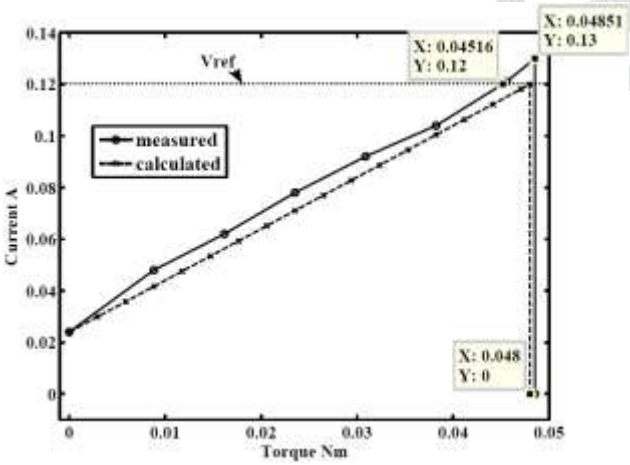

(b)

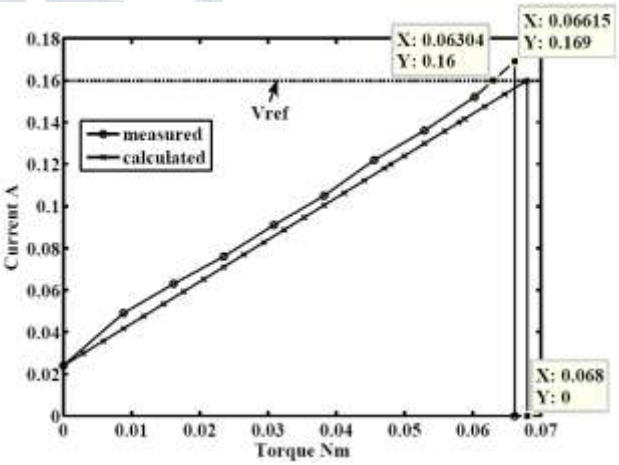

(d)

Figure 7: The experimental and calculated result with different reference voltages (a) 100 mV; (b) 120 mV; (c) 140 mV and (d) 160 mV.

Figure 7 shows the performance of the driver circuit with 100mV, 120mV, 140mV and 160mV reference voltages respectively, and there is little variation in practically observed and calculated values. For reference voltage 100mV, the motor should stop at 100mA motor current, which correspond to a torque of 0.035Nm at the motor shaft, but the measured value of the armature current is 110mA at which the motor stopped, which correspond to a torque of 0.041Nm. The difference in the measured values and calculated values of the armature current, which stops the motor, is due to the delay generated by the program, executed inside the microcontroller, to accommodate starting surge current of the motor. Also, due to the motor losses, the observed torque is little less than the calculated torque at same armature current.

By using the H-bridge motor driver in place of MOSFET driver, the direction of rotation of the motor can also be controlled. Hence this driver circuit could be applicable in pick and place robotic action [28-29]. How et al. [24] reported a modular motor driver with torque control for gripping mechanism. They used the PWM signal to control the torque of the DC motor using Arduino UNO microcontroller. The designed SCS circuit can also be used with other type of smart actuators such as shape memory alloy actuator [30]. Kim et al. [31] presented a short circuit controller for use in the humidification of polymer electrolyte membrane fuel cell and also showed the effect of controlling speed of cooling fans and purging period of purging valve. By applying the SCS technique in their presented work, the speed of the cooling fan, hydrogen purging period and short circuit period could be controlled as the FC stack current increased from a set value and this would reduce the power consumption of the fuel cell system.

V. Conclusions

A self current sensing intelligent DC motor drive using embedded system technology is successfully designed and tested. First of all, the characteristic of the actuator has observed to find out it's some measurable parameter that could use as sensing information. In this present work, the circuit has designed and verified with 12V, permanent magnet brushed DC motor with gearbox. Hence, the no-load and stall characteristic of the motor has firstly demonstrated. A low-side current sensing resistance R_{sense} has used to sense the motor current with an on chip analog comparator of the controller, to compare the sensed motor current with the reference value. The whole system was powered with general purpose battery, which limits the circuit working duration and needed change for several times with new. In case of the rechargeable battery, frequent recharging is required. Hence the use of fuel cell power system would be the best option for long operational duration with efficient and clean mechanism. This circuit could be used in any DC motor based industrial, robotic or smart systems where gripping, end point detection or overload current protection is required. This circuit is simple and cost effective since a resistance with low value is used to sense the motor current with a controller having an on chip analog comparator.

References

[1] Ormaechea LMC. Humanoid Robots. In: Rodríguez NEN. Editor. Advanced Mechanics in Robotic Systems. Springer; 2011: 1-18.
[2] Pellicciari M, Berselli G, Leali F, Vergnano A. A method for reducing the energy consumption of pick-and-place industrial robots. Mechatronics. 2013; 23: 326–334.
[3] Crisp D, Pathareb A, Ewell RC. The performance of gallium arsenide/germanium solar cells at the Martian surface. Progress in Photovoltaics Research and Applications. 2004; 54: 83-101.
[4] Thangavelautham J, Strawser D, Dubowsky MYCS. Lithium Hydride Powered PEM Fuel Cells for Long-Duration Small Mobile Robotic Missions. IEEE International Conference on Robotics and Automation (ICRA). 14-18 May 2012.
[5] Kamarudina SK, Achmada F, Dauda WRW. Overview on the application of direct methanol fuel cell (DMFC) for portable electronic devices. International journal of hydrogen energy. 2009; 34: 6902 – 6916.
[6] Wilberforce et al. Advances in stationary and portable fuel cell applications. International journal of hydrogen energy. 2016; 1–14.
[7] Sharaf OZ, Orhan MF. An overview of fuel cell technology: Fundamentals and applications. Renewable and Sustainable Energy Reviews. 2014; 32: 810-853 .
[8] Mekhilefa S, Saidurb R, Safari A. Comparative study of different fuel cell technologies. Renewable and Sustainable Energy Reviews. 2012; 16: 981-989.
[9] Vaghari H, Jafarizadeh-Malmiri H, Berenjian A, Anarjan N. Recent advances in application of chitosan in fuel cells. Sustainable Chemical Processes. 2013; 1–16.
[10] Kordesch K. Alkaline fuel cells applications, innovative energy technology. Austria: Institute of High Voltage Engineering, U Graz; 1999.
[11] Hoogers G. Fuel cell technology handbook. In Edited by Hoogers G. Boca Raton: FL: CRC Press; 2003:8–39.
[12] Ramirez-Salgado J. Study of basic biopolymers as proton membrane for fuel cell systems. Electrochim Acta. 2007, 52: 3766–3778.
[13] Larminie J. Fuel Cell Systems Explained Second Edition. 2003.
[14] Bullen RA, Arnot TC, Lakeman JB, Walsh FC. Biofuel cells and their development. Biosens-Bioelectron. 2006; 21: 2015-45.
[15] Shukla AK, Suresh P, Berchmans S, Rajendran A. Biological fuel cells and their applications. CurrSci. 2004; 87: 455-68.
[16] Taro et al. PEFC Deep Cruising AUV URASHIMA. Fuel Cell Symposium Proceedings. 2003; 90-95.
[17] Joh et al. A direct methanol fuel cell system to power a humanoid robot. Journal of Power Sources. 2003; 195: 293-298.
[18] Kesner et al. Mobility and Power Feasibility of a Microbot Team System for Extraterrestrial Cave Exploration. Proceedings of the IEEE International Conference Robotics and Automation. Rome, Italy. 2007.
[19] Lee, et al. Development of a 600 W Proton Exchange Membrane Fuel Cell Power System for the Hazardous Mission Robot. Journal of Fuel Cell Science and Technology. 2010; 310061-310067.
[20] Wang Q, Lan Z. The application prospect of fuel cell for the rehabilitation aids. International journal of hydrogen energy. 2016; 41: 15777-15782.
[21] Wilhelm AN, Surgenor BW, Pharoah JG. Design and Evaluation of a Micro-Fuel-Cell-Based Power System for a Mobile Robot. IEEE/ASME Transactions on Mechatronics. 2006; 11(4): 471-476.
[22] Randazzo et al. A comparison between joint level torque sensing and proximal F/T sensor torque estimation: implementation on the iCub. IEEE/RSJ International Conference on Intelligent Robots and Systems (IROS). 25-30 Sept. 2011.
[23] Kazemi M, Valois JS, Bagnell JA, Pollard N. Human-inspired force compliant grasping primitives Auton Robot. 2014; 37: 209–225.
[24] How et al. Modular Motor Driver with Torque Control for Gripping Mechanism. Procedia Engineering. 2012; 41: 1476 – 1482.
[25] Hanson B, Levesley M. Self-sensing applications for electromagnetic actuators. Sensors and Actuators A. 2004; 116: 345–351.
[26] Zhen Y. Current Sensing Circuit Concepts and Fundamentals, Microchip Technology Inc, 2011.

[27] Lepkowski J. Motor Control Sensor Feedback Circuits, Microchip Technology Inc, 2003.
[28] Jin et al. Minimal Grasper: A Practical Robotic Grasper With Robust Performance for Pick-and-Place Tasks. IEEE Transactions on Industrial Electronics. 2013; 60(9). 3796-3805.
[29] Daoud S, Chehade H, Yalaoui F, Amodeo L. Efficient metaheuristics for pick and place robotic systems optimization. J Intell Manuf. 2014; 25: 27–41.
[30] Ruth DJS, Nakshatharan SS, Dhanalakshmi K. Differential resistance feedback control of a self-sensing shape memory alloy actuated system. ISA Transactions. 2014; 53: 289–297.
[31] Kim et al. Humidification of polymer electrolyte membrane fuel cell using short circuit control for unmanned aerial vehicle applications. International journal of hydrogen energy. 2014; 39(15): 7925–7930.